Probing the subsurface karst features using time-frequency decomposition[a]

[a]Published in Interpretation, 4, No.4, T541-T550, (2016)

Yangkang Chen[1]

ABSTRACT

The high-resolution mapping of karst features is of great importance to hydrocarbon discovery and recovery in the resource exploration field. However, currently, there are few effective methods specifically tailored for such mission. The 3D seismic data can reveal the existence of karsts to some extent but cannot obtain a precise characterization. I propose an effective framework for accurately probing the subsurface karst features using a well-developed time-frequency decomposition algorithm. More specifically, I introduce a frequency interval analysis approach for obtaining the best karsts detection result using an optimal frequency interval. A high resolution time-frequency transform is preferred in the proposed framework to capture the inherent frequency components hidden behind the amplitude map. Although the single frequency slice cannot provide a reliable karst depiction result, the summation over the selected frequency interval can obtain a high-resolution and high-fidelity delineation of subsurface karsts. I use a publicly available 3D field seismic dataset as an example to show the performance of the proposed method.

INTRODUCTION

Karst is a type of solutional caves that are usually formed in soluble rock limestone when an aggressive fluid dissolves the rock. Subsurface karsting can produce a range of different structures, such as widened fissures and different types of cavities at all scales. These may locally be partly or completely filled by speleothems, sediments deposited by streams or breccia derived from stoping or collapse of the cave roof and walls (Nordli, 2009). Commonly known karst features are fluid-enhanced faults (Nissen et al., 2005), eroded caves, and sinkholes. The karst features are usually related with big petroleum reservoirs (Ford and Williams, 1989). Understanding the spatial distribution of the karsts is of great importance to the discovery of hydrocarbons and their optimal recovery from these reservoirs. However, this can be very difficult due to several reasons. One reason is that the karsts are not uniformly distributed and exhibit an extreme spatial variability. Another reason is that the karst features are usually below seismic resolution, which makes them difficult to map. In this paper,

I propose a high-resolution characterization approach for mapping the karst features by utilizing time-frequency decomposition of 3D seismic data.

Time-frequency decomposition offers extra information when analyzing seismic data, which has been extensively used in seismic data processing and interpretation (Han and van der Baan, 2013; Reine et al., 2009; Rodriguez et al., 2012; Fomel, 2013; Zhang et al., 2015a; Chen et al., 2015; Liu et al., 2016b; Zhang et al., 2016). One of the most commonly used applications of time-frequency analysis is that deeper channels are usually of stronger amplitude at lower frequency in the time-frequency map, and the shallower flank of the channel has larger amplitude at higher frequencies in the time-frequency map (Liu et al., 2016c; Cheng et al., 2016; Liu et al., 2016a). In addition, time-frequency analysis can be used in estimating attenuation, pore-pressure prediction, detecting seismic unconformities, and some implementation of seismic chronostratigraphy (Lin et al., 2013). Over the past decades, time-frequency decomposition has found a panoply of applications in seismic data processing and interpretation (Liu and Marfurt, 2007). Most time-frequency decomposition approaches are used in detecting low-frequency shadow (Castagna et al., 2003), detecting paleochannels (Liu et al., 2011a), reservoir characterization (Zhang et al., 2015b), structural and stratigraphic delineation (Liu et al., 2016c; Chen et al., 2016), arrivals picking of P or S wave modes (Pinnegar and Mansinha, 2003). In this paper, I propose an application of the time-frequency decomposition in probing the subsurface karst features. Four approaches with different analyzing resolutions are compared to offer more practical guidelines for utilizing the proposed approach.

Some researchers have mentioned the application of time-frequency decomposition approaches in delineating the subsurface karst feature, but most applications are not introduced in detail (Chopra and Marfurt, 2007; Fisher et al., 2010). The karst features are depicted based on the criteria that they are discontinuous in spatial domain and show frequency anomalies. The challenge in delineating karst feature lays in the fact that high-resolution delineation may result in many spurious frequency anomalies while low-resolution delineation may fail to depicted such valuable details. A method that can offer us freedom to control the characterization resolution and fidelity is in strong demand.

METHOD

Time-frequency decomposition maps a 1-D signal in the time domain into a 2-D image in time-frequency space, which can describe the local time-frequency variations of geophysical properties. There have been many different approaches for such decomposition mission, such as the continuous wavelet transform (Daubechies, 1992), S transform (Stockwell et al., 1996), and synchrosqueezing wavelet transform (Daubechies et al., 2011). I will not promote a new algorithmic advance here for better time-frequency decomposition, but instead, I will propose a novel and effective way for mapping the subsurface karst features based on a simple frequency interval analysis approach using 3D seismic data recorded at the surface of the targeted area.

The algorithm can be summarized in three simple steps:

- Step 1: Input the 3D seismic data, and define the minimum and maximum analyzing frequency $\omega_{\min}$ and $\omega_{\max}$ and frequency interval distance $\Delta\omega$.
- Step 2: Apply time-frequency decomposition to each trace of the 3D seismic data and sum the frequency components in each frequency interval $< \omega_i, \omega_i + \Delta\omega >$, $i = 1, 2, \cdots, N$, where N denotes the number of frequency intervals, then reform the summed frequency components of different intervals into several 3D cubes that correspond to different frequency intervals.
- Step 3: Output the different frequency cubes and analyze the results to pick the best frequency interval that can best depicts the karst features.

$\omega_{\min}$ and $\omega_{\max}$ are chosen based on the bandwidth of seismic data. A reference value can be $\omega_{\min} = 1$Hz and $\omega_{\max} = 100$Hz. The $\Delta\omega$ is the only parameter that may need several trials. One can test the $\Delta\omega$ from 5Hz to 30 Hz, and updating $\Delta\omega$ every 5Hz. The choice of $\Delta\omega$ is a compromise between analysis complexity and the characterization resolution.

It is worth mentioning that time-frequency based karst delineation approach is not new in geophysical study. A typical and standard way to extract subsurface karst features based on time-frequency decomposition is to extract different constant frequency slices, and then to select a certain frequency slice to best represent the karst features based on a prior knowledge and good correlation between the frequency slice and the amplitude map. However, the single frequency slice depiction is sometimes not reliable since higher frequency may provide fine-scale delineation with higher resolution, while lower-frequency may provide large-scale result with lower resolution. The result of the contradiction in traditional approaches is that there might be spurious bright spots or unclear karsts representation. I will just mention the problem here and will show it in detail in the data example. The frequency interval analysis approach provides us a convenient way to control the resolution and reliability of finally depicted karsts by simply adjusting the frequency interval. Although determining the frequency interval still requires some efforts in its current version, my experience shows that frequency interval is usually chosen as 5, 10, or 20Hz.

STUDY AREA AND DATASET

The studied dataset is a 3D dataset that was a significant part of the total data base amassed during a two-year study of the Bend Conglomerate reservoir system in Boonsville Field in north-central Texas. The 3D Boonsville field dataset (Hardage et al., 1996b,a) was made publicly available for educational training purposes for a broad range of industry and academic interests since 1996 by Bob Hardage from the Bureau of economic Geology at The University of Texas at Austin. A special property of this dataset is that it shows interesting karst phenomenon of deep Ellenburger

carbonates, which generate collapse structures that have compartmentalized clastic Bend Conglomerate reservoirs 620 to 760 meters above the depths where collapse structures originate. The demonstration of the study area is shown in Figure 1. Figure 2 shows the strati-graphic column of the Fort Worth Basin (Pollastro et al., 2007). The formation of interest is the Ordovician-age Ellenburger carbonate section. The Ellenburger carbonate section creates near-vertical chimneys-like karst collapses.The 3D seismic dataset is shown in Figure 3 and a selected 2D profile (crossline=75) is shown in Figure 5a. It can be observed that around the depth of 1.25s, there are some karst collapses, which is however, not very clear. In the next section, I will show a much better delineation result using time-frequency decomposition.

Some structure-related anomalies, such as the faults, discontinuities, karst collapses, are not always easily viewed from the original amplitude-based seismic profile. There are many approaches in the literature which better highlights the structural anomalies. One of the most common methods is to define a new seismic attribute which is sensitive to the structural anomalies (Wang et al., 2015; Xie et al., 2015b). The 3D dataset from the Boonsville field contains typical karst phenomenon, as shown in Figures 3 and 5a. But, from the original seismic reflections, the phenomenon is not obvious.

RESULTS

By utilizing the proposed frequency interval analysis method, one can divide the total frequency range into different sub-bands, and analyze the structural behaviors delineated from the sub-bands. In this paper, I use the synchrosqueezing wavelet transform (SSWT) (Daubechies et al., 2011; Chen et al., 2014; Xie et al., 2015a) for the time-frequency delineation of the karsts. I let $\omega_{\min} = 1$Hz, $\omega_{\max} = 80$Hz, and $\Delta\omega = 20$Hz, which is the optimal parameter combination for this dataset. I choose $\omega_{\min} = 1$ Hz and $\omega_{\max} = 80$ Hz by looking at the averaged frequency spectrum of the seismic data and finding out that amplitude spectrum beyond 80 Hz or below 1 Hz is almost negligible. $\Delta\omega = 20$Hz is decided by comparing the delineation results (as shown in Figure 4b) with $\Delta\omega = 5, 10, 20$ Hz, respectively, and founding out that $\Delta\omega = 20$Hz gives the best performance. The four 3D cubes that correspond to four different frequency intervals ($< 1, 20 >$ Hz, $< 21, 40 >$ Hz, $< 41, 60 >$ Hz, and $< 61, 80 >$ Hz) are shown in Figures 4a to 4d, respectively. Focusing on the target layer from 1.0 s to 1.4 s, it is obvious that the result of the frequency interval $< 21, 40 >$ clearly shows the distribution of the karsts. Please note that the closer the color is to blue, the higher possibility that area is karst. The collapsed karsts are not formed during continuous sedimentation and thus is usually composed of complicated components. There are no layered structures inside the karsts, which will make seismic wave go through a strong scattering process when traveling through the karst media. The strong scattering will be revealed in seismic image as discontinuities, which will be further revealed in time-frequency maps as low amplitude phenomenon in the dominant frequency range. Thus, the blue (close to zero) is of higher likehood of

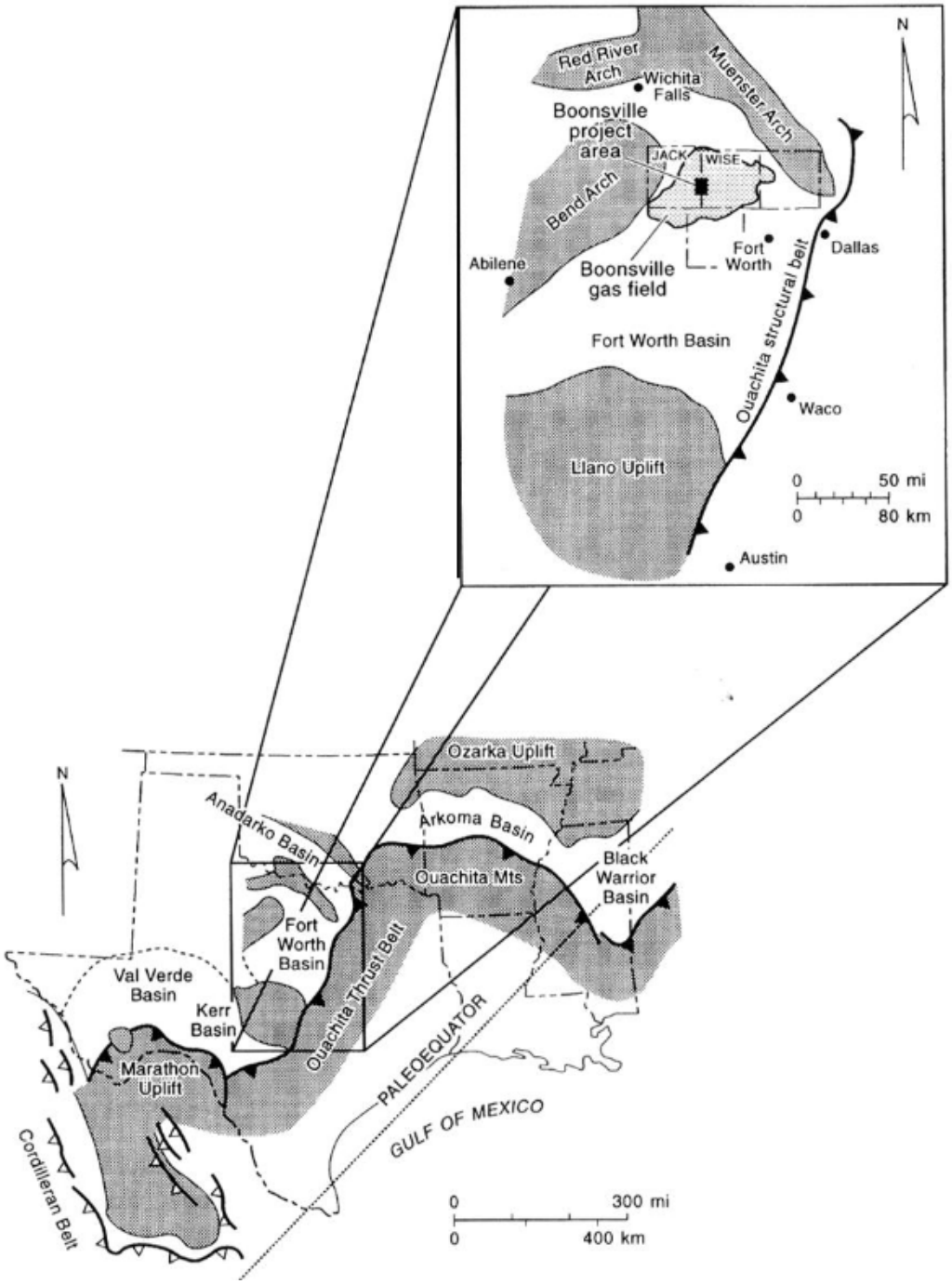

Figure 1: Middle Pennsylvanian paleogeographic map showing the Fort Worth Basin and other basins related to the Ouachita orogony and the Boonsville project area. The solid rectangle on the Wise-Jack county line designates the site of the 3-D seismic survey, curtersy of Hardage et al. (1996b).

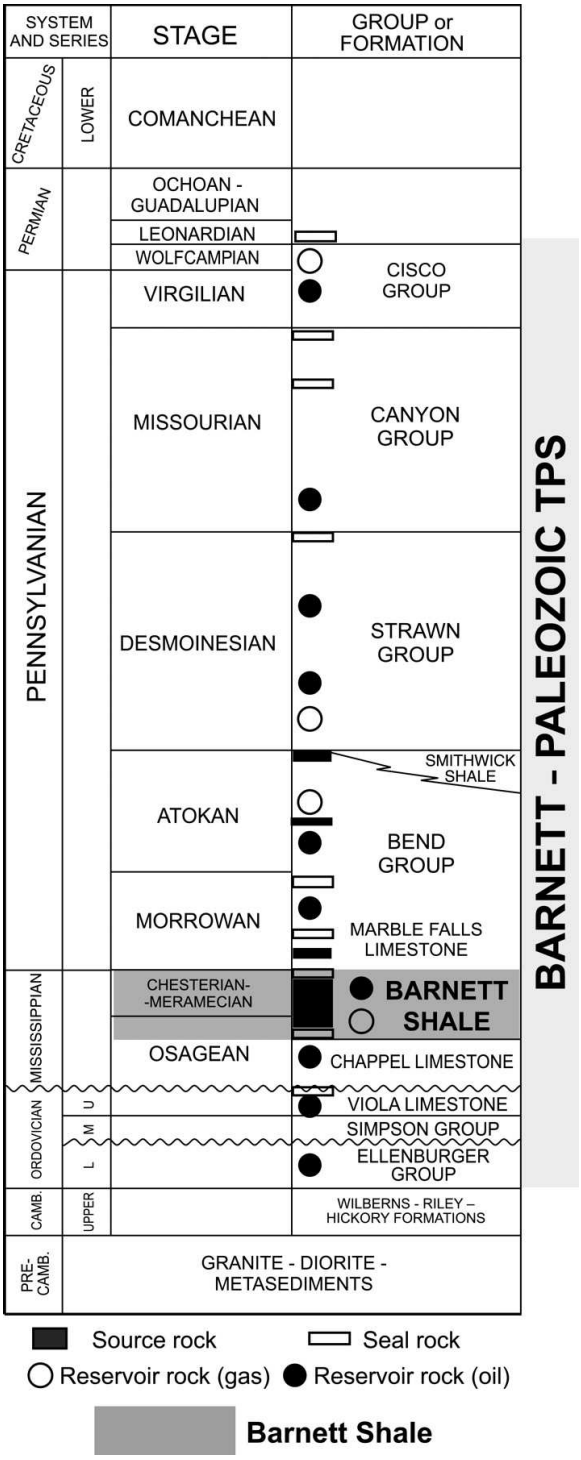

Figure 2: Strati-graphic column of the Fort Worth Basin, curtersy of Pollastro et al. (2007). The target horizon is the deep Ordovician-age Ellenburger carbonate section which causes numerous karst collapses and significant disruptions in the overlaying strata.

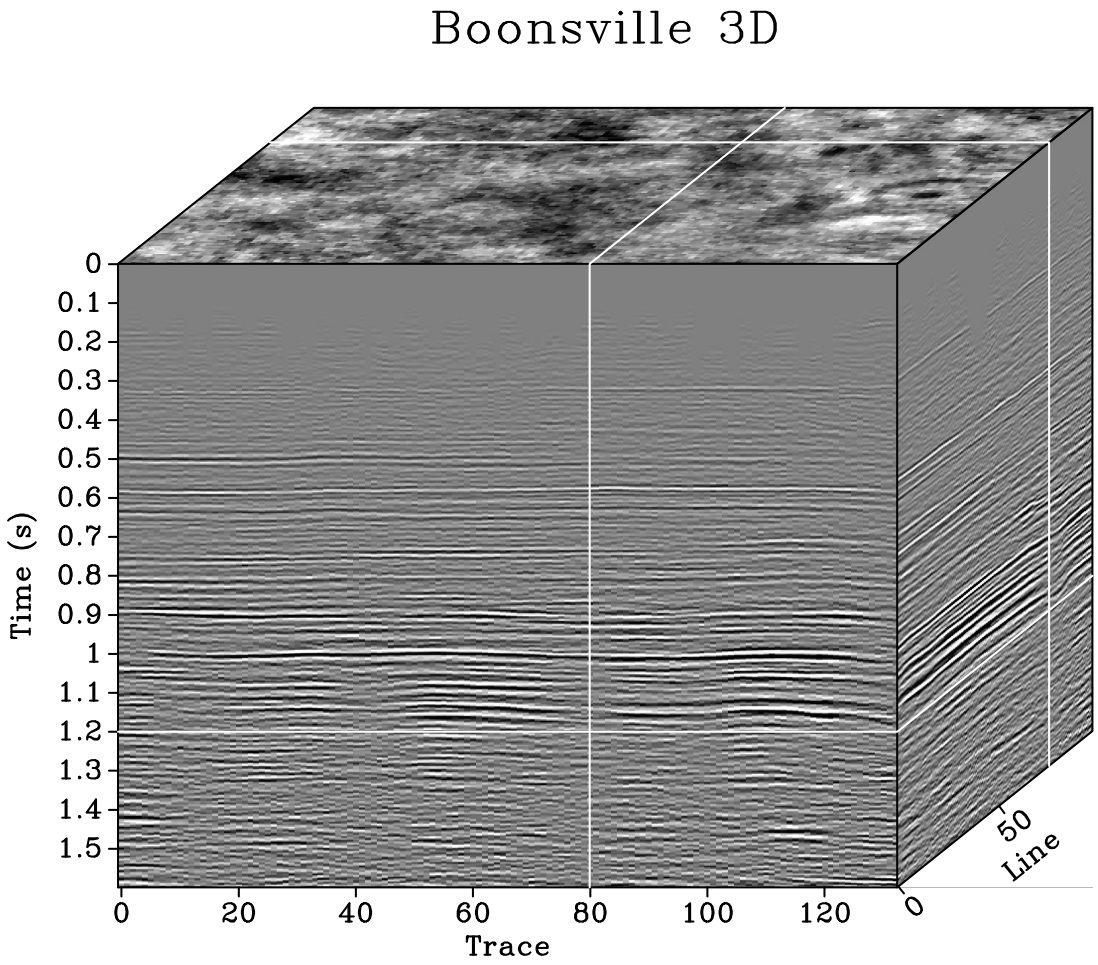

Figure 3: 3D Boonsville dataset after time migration.

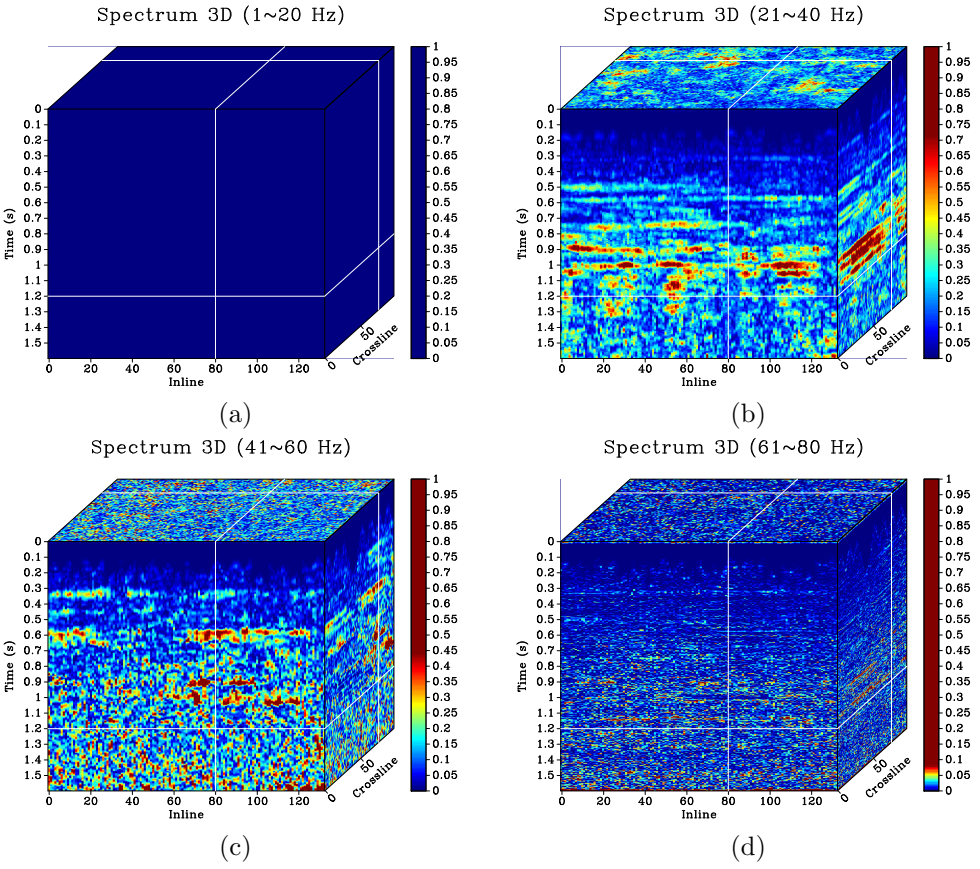

Figure 4: 3D karst features delineation result using SSWT with different frequency intervals.

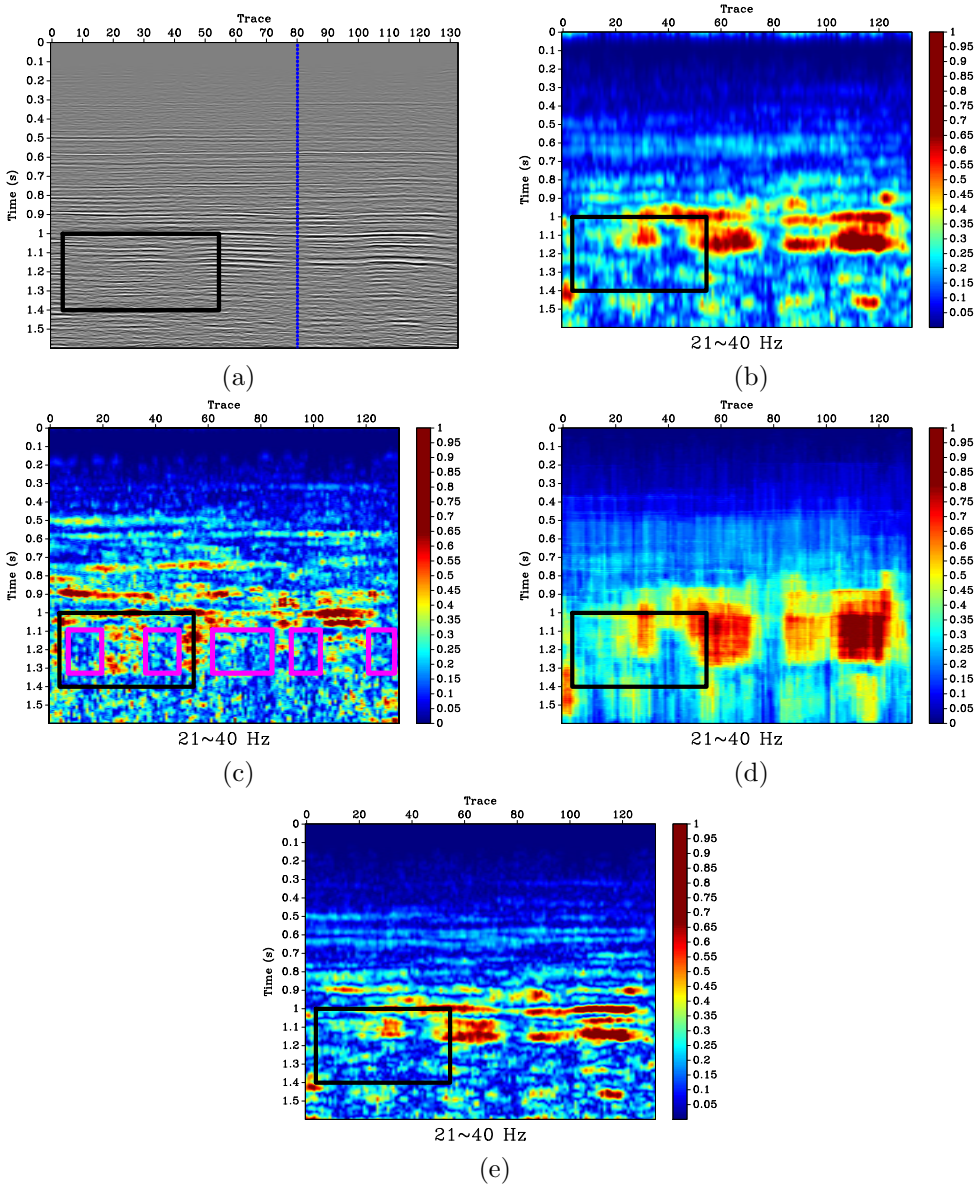

Figure 5: 2D seismic section (crossline=75) and its karst mapping results. (a) Amplitude section. (b) Low frequency slice of ST. (c) Low frequency slice of SSWT. (d) Low frequency slice of STFT. (e) Low frequency slice of LTFT.

karst. I then select the best 3D karst characterization result of the frequency interval $< 21, 40 >$ Hz and show it in detail in Figure 9 and will discuss about the details later.

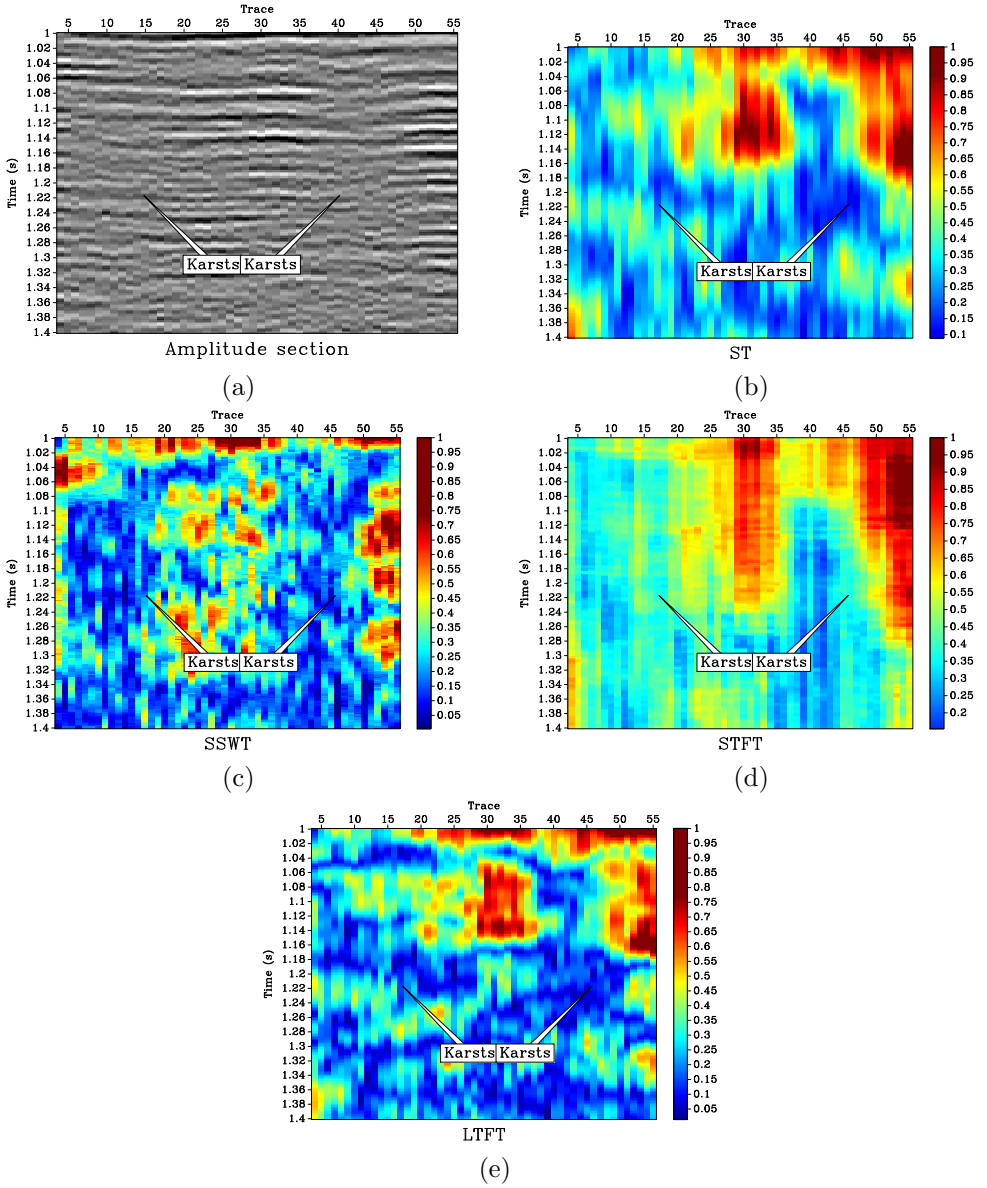

Figure 6: Zoomed 2D seismic section (crossline=75) and its zoomed karst mapping results. (a) Amplitude section. (b) Low frequency slice of ST. (c) Low frequency slice of SSWT. (d) Low frequency slice of STFT. (e) Low frequency slice of LTFT.

I then take the selected 2D section for further analysis. I compare the performance using four different time-frequency decomposition approaches: the S transform, the SSWT transform, the short time Fourier transform (STFT), and the local attribute based time-frequency transform (LTFT) (Liu et al., 2011b) . The delineation results using ST, SSWT, STFT, and LTFT are shown in Figures 5b, 5c , 5d , and 5e , respectively. The result from SSWT is very appealing because those karst collapses

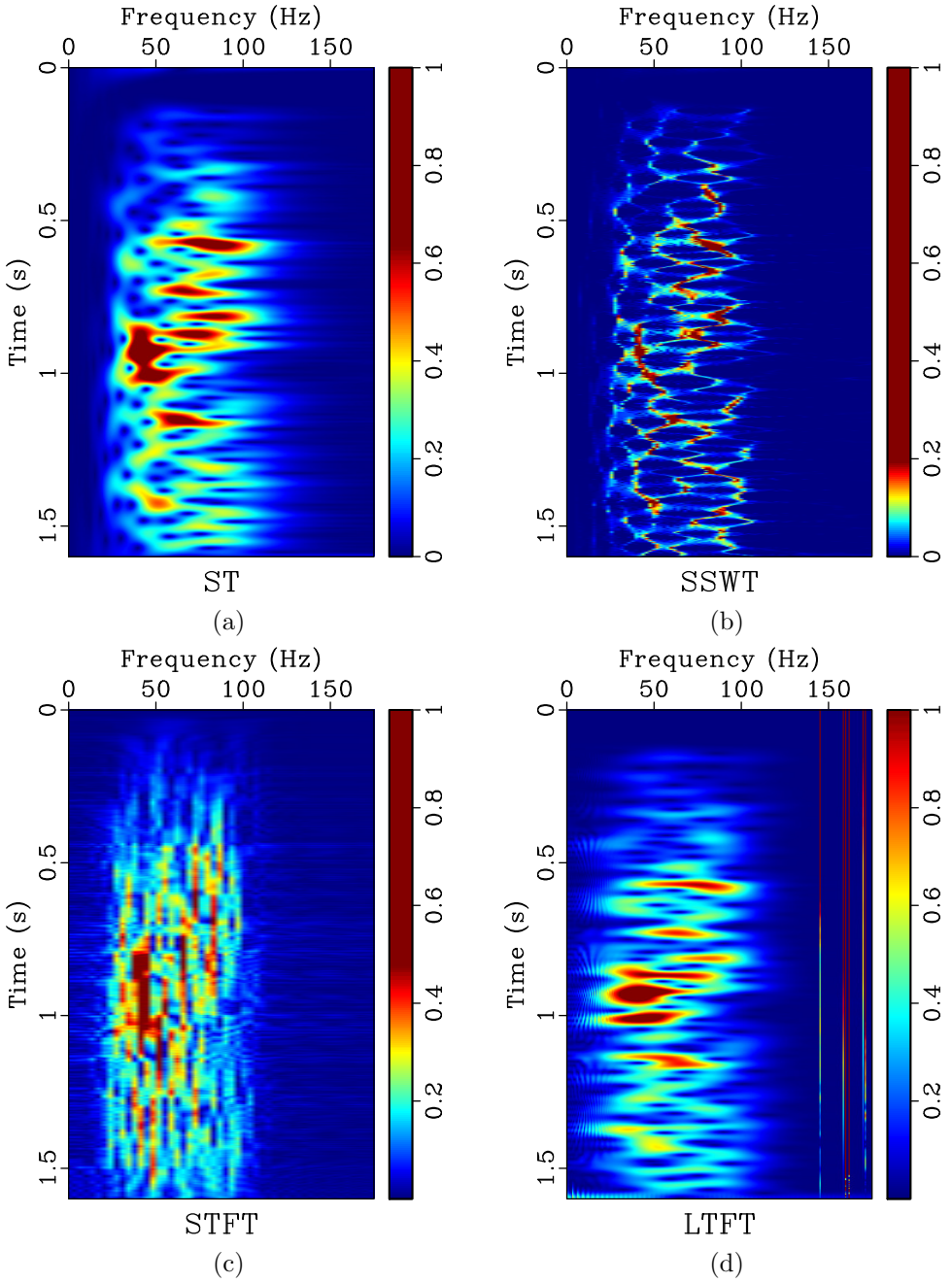

Figure 7: Time-frequency maps of the 80th trace in the 2D seismic section as shown in Figure 5a, using (a) ST and using (b) SSWT. (c) STFT. (d) LTFT. The selected trace is highlighted by the blue line in Figure 5a.

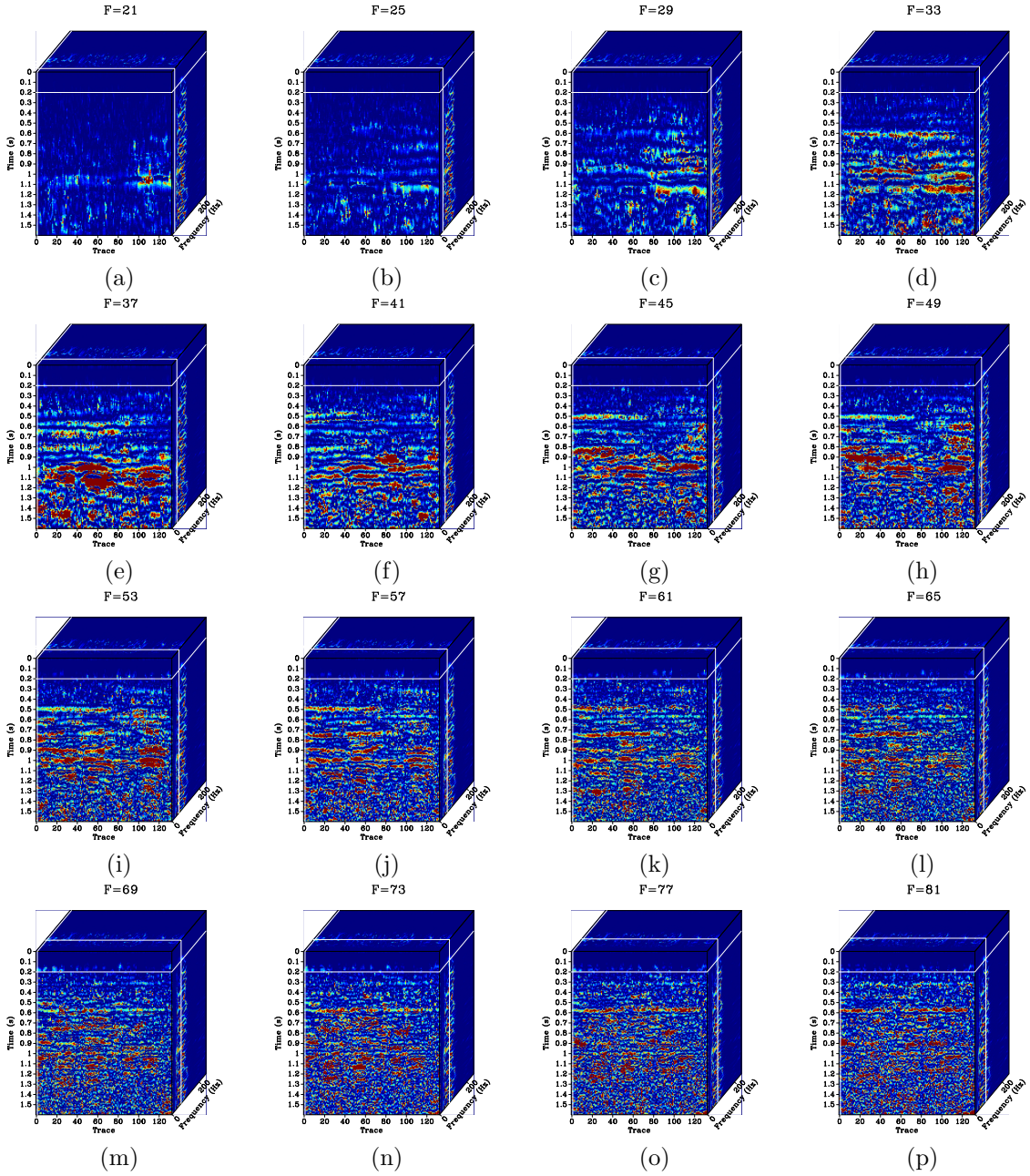

Figure 8: Constant frequency slices using SSWT. The frequency range is from 21 to 81 Hz. Frequency interval is 4 Hz.

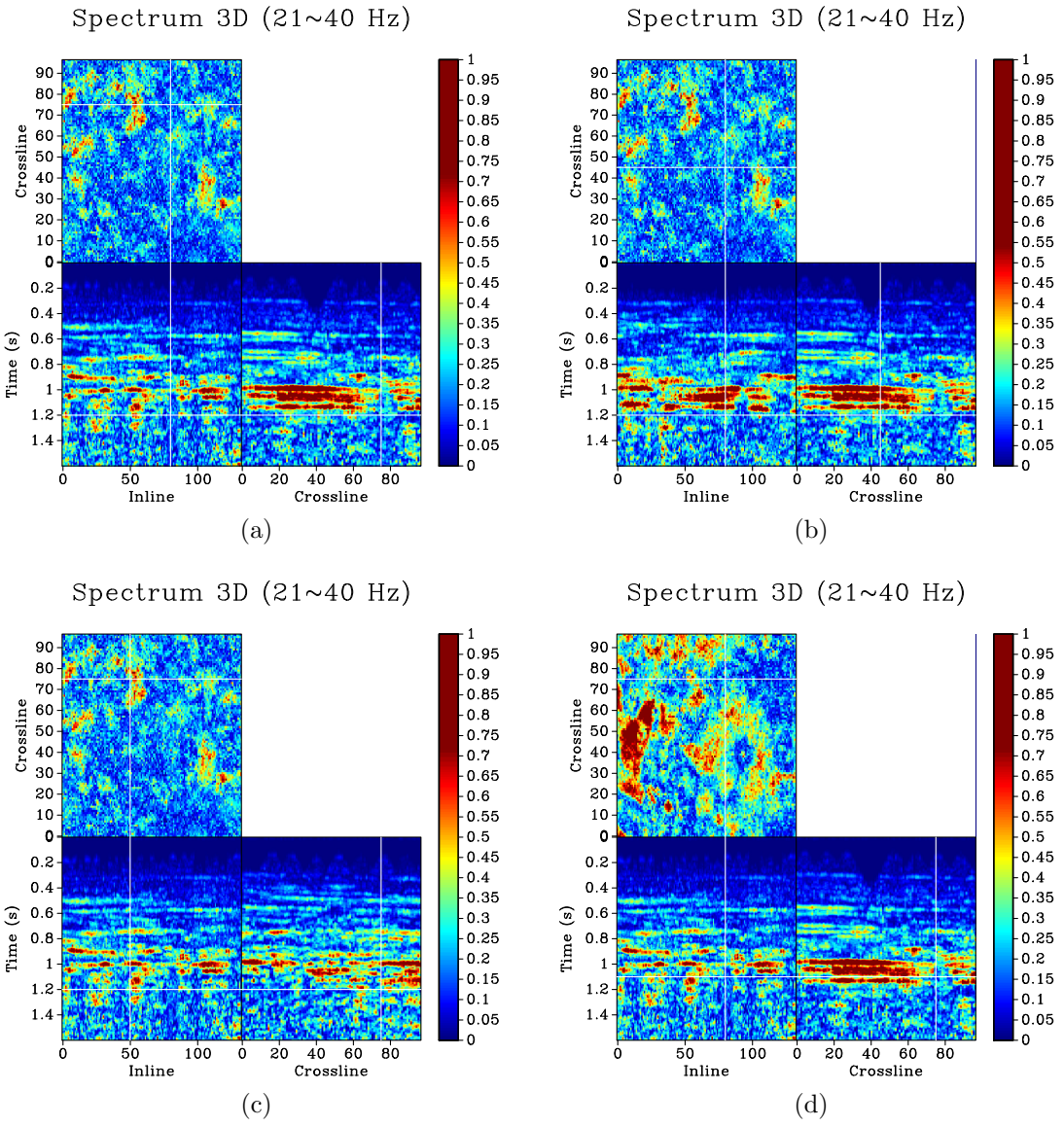

Figure 9: 3D karst features mapping results (flat view) using SSWT with different time (top), crossline (left) and inline (right) slices. (a) Crossline=75, inline=80, time=1.2s. (b) Crossline=45, inline=80, time=1.2s. (c) Crossline=75, inline=50, time=1.2s. (d) Crossline=75, inline=80, time=1.1s.

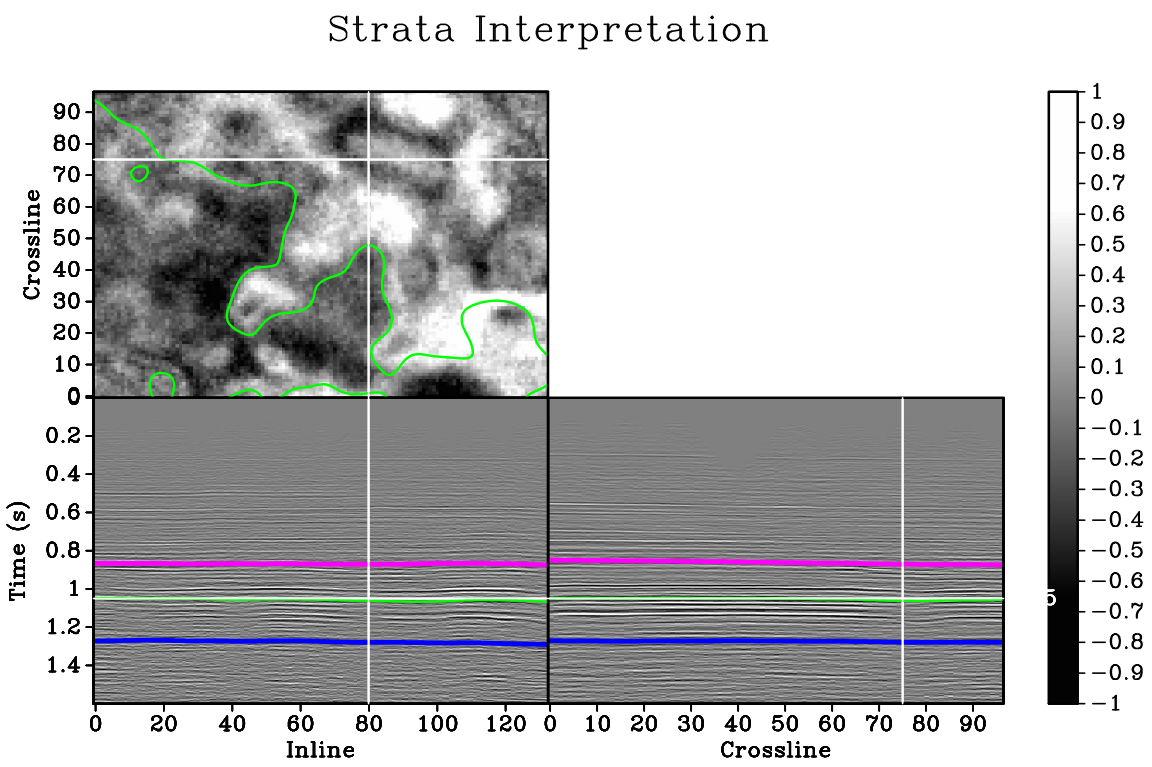

(a)

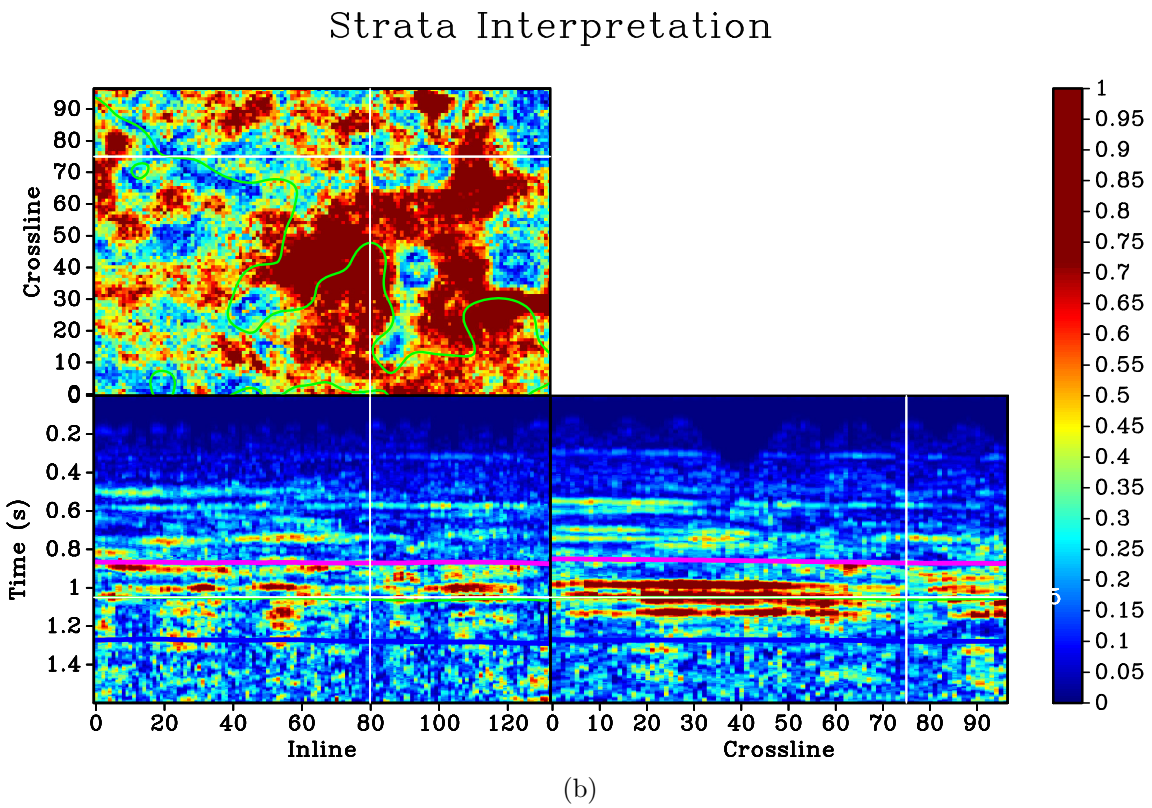

(b)

Figure 10: Different strata slices from the time-frequency delineation result, shown in Figure 10b. (a) Top of Caddo. (b) Strata slice between Caddo and Vineyard. (c) Top of Vineyard. (d) Strata slice between Vineyard and the base.

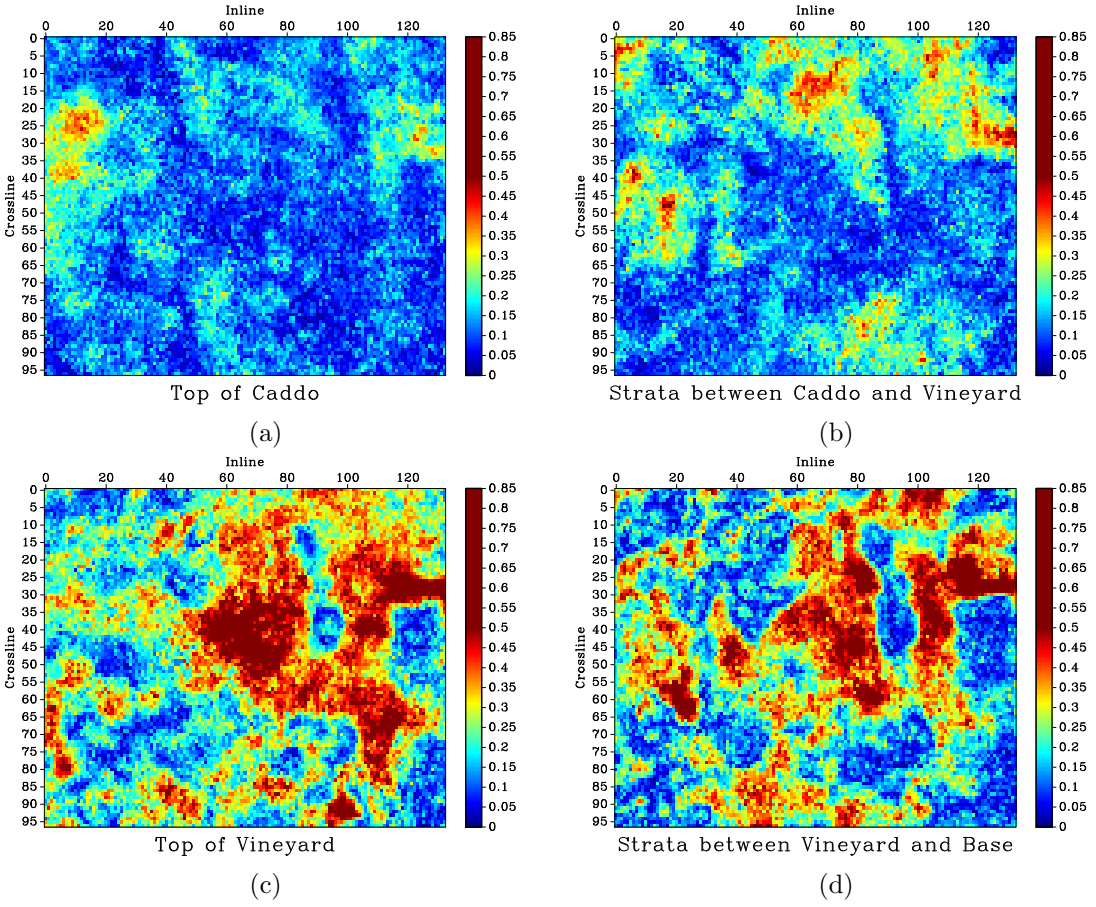

Figure 11: Different strata slices from the time-frequency delineation result, shown in Figure 10b. (a) Top of Caddo. (b) Strata slice between Caddo and Vineyard. (c) Top of Vineyard. (d) Strata slice between Vineyard and the base.

are all depicted by the time-frequency decomposition (see those pink frame boxes), and the collapse areas are all corresponding to small amplitude in the low frequency slice. However, all other time-frequency transforms cannot decompose the seismic data in such way. In order to make the comparison clearer, I zoom a part from each figure in Figure 5 and show them in Figure 6. The zoomed area is highlighted by the black frame boxes in Figure 5. In Figure 6, the blue color in Figure 6c correlates well with the collapsed area in Figure 6a. The best mapping of karsts using SSWT is due to its high resolution property when analyzing 1D non-stationary seismic signals. Figure 7 shows time-frequency decomposition results of the 80th trace of the 2D seismic section as shown in Figure 5a, using four different approaches (ST, SSWT, STFT, and LTFT). The selected trace is highlighted by blue in Figure 5a. From the comparison, one can see that SSWT has a much higher frequency resolution than ST, STFT, and LTFT. From the single-trace time-frequency slice one can judge roughly in which depth the data show abnormal frequency, and what their corresponding dominant frequency components are. In order to show superior performance of the frequency interval analysis approach as introduced in this paper, over the traditional single frequency slice analysis approach, I plot 16 single frequency slices in Figure 8. The frequency range is from 21 Hz to 81 Hz, and I plot the frequency slices every 4 Hz. It can be observed that the time-frequency decomposition results of subsurface properties are either of too low resolution, as shown in the low frequency slices, or of too high resolution as shown in high frequency slices.

Figure 9 shows 3D karst delineation results (flat view) using SSWT with different time (top), crossline (left) and inline (right) slices. Figure 9a differs from 9b by different crossline sections. From the comparison between Figures 9a and 9b, one can see clearly how the karst varies along the crossline direction: the karst becomes weaker from crossline 75 to crossline 50. In the same way, one can study the karst variation along the inline direction by comparing Figures 9a and 9c. It is also possible to evaluate the volume of the karst controlled area by looping along different directions in the 3D volume (Figure 4b), which is closely related with the karst controlled reserve. Figure 10a shows an interpreted 3D seismic section with three key stratas highlighted. The top pink line, middle green line, and bottom blue line denote the Caddo strata, the Vineyard strata, and the Ellenburger strata, respectively. Figure 10b shows the time-frequency delineation result of the karsts overlaid by the picked three horizons. The Upper Caddo is the top boundary of the productive Bend Conglomerate section, and the Upper Vineyard is a sequence near the base of the Bend Conglomerate section. The Bend Conglomerate section is of Middle Pennsylvanian age (also known as Atokan) and is targeted throughout the 1980s and 1990s as it contains several oil&gas bearing reservoirs. The thickness is around 300-360 meters in this area, with a depth from 1370 to 1830 meters (Hardage et al., 1996b,a). It can be observed from the karsts mapping result shown in Figure 10b that the karsts spreads a deep range from the Upper Caddo to the base of Ellenburger. I also selected different strata slices from Figure 10b and show them in Figure 11. Figure 11a shows a structure surface of the top of Caddo. Figure 11b shows a structure surface between Caddo and Vineyard. Figure 11c shows a structure surface on the top of Vineyard.

Figure 11d shows a structure surface between Vineyard and the base of Ellenburger carbonate section. It can be observed that from up to down, the main color turns from cool (blue) to warm (red), indicates that the karstification weakens as the depth increases, which is consistent with the fact that the consolidation becomes stronger as the depth increases and make the deeper strata has stronger collapses and less karsts.

The Boonsville 3D dataset consolidate the proposed frequency interval analysis method in delineating subsurface karst collapses. When I use the term *karst collapses*, I intend to refer to all those commonly seen karst features, such as incised valleys, eroded caves, sinkholes, and so on. While the reasons causing these karst features are different, they will all cause more or less depressions or collapses to the overburden strata and have a similar situation as the one presented in the Boonsville example. There is a large potential that the proposed framework can be successfully used in any type of karst features, and future validation of the framework on more field datasets are worth being done. The sediment or mud-filled collapse features may not cause significant differences of anomalies in amplitude spectrum and they will both show irregularities on the 3D seismic images since seismic wave will experience strong scattering effects when traveling through the collapsed area. But future investigation should be done to validate this inference.

CONCLUSION

Accurate mapping of karst features is crucial for the resources exploration and recovery. The 3D seismic data can offer some insights in the spatial distribution of the karsts, but with low resolution, since the boundary of karst caves cannot be clearly delineated and the small-scale kart features are smeared in the seismic reflections. I propose to use time-frequency decomposition via a frequency interval analysis approach to accurately map the subsurface karst features with high resolution and accuracy. The time-frequency resolution can affect the final depicted result, and I suggest using the high-resolution synchrosqueezing wavelet transform (SSWT) to perform such task. The frequency interval analysis approach can provide us with more freedom in controlling the resolution and reliability of the final depicted result, compared with the traditional single frequency slice based approach. The proposed method is easy to implement and deserves more attention to assist in geological research on the topic of karst evolution.

ACKNOWLEDGEMENTS

I would like to thank Summer Li, Qian Xie, Shuwei Gan, Wei Liu, Zixiang Cheng, Tingting Liu for helpful discussions, and Bob Hardage for making the Boonsville dataset publicly available. I also thank associate editor Hongliu Zeng, Victor Aarre, and two anonymous reviewers for constructive suggestions that improved the manuscript greatly. Finally, thanks to Dmytro Iatsenko for sharing the SSWT code online:

http://www.physics.lancs.ac.uk/research/nbmphysics/diats/tfr/.

REFERENCES

Castagna, J., S. Sun, and R. W. Siegfried, 2003, Instantaneous spectral analysis: Detection of low-frequency shadows associated with hydrocarbons: The Leading Edge, **22**, 120–127.

Chen, Y., S. Li, G. Zhang, and S. Gan, 2015, Delineating karstification using synchrosqueezeing wavelet transform: SEG expanded abstracts: 85th Annual international meeting, 1835–1840.

Chen, Y., T. Liu, X. Chen, J. Li, and E. Wang, 2014, Time-frequency analysis of seismic data using synchrosqueezing wavelet transform: Journal of Seismic Exploration, **23**, 303–312.

Chen, Y., W. Liu, G. Zhang, Z. Cheng, and W. Chen, 2016, Seismic time-frequency anlysis using improved complete ensemble empirical mode decomposition: 78th Annual International Conference and Exhibition, EAGE, Extended Abstracts.

Cheng, Z., Y. Chen, W. Liu, G. Zhang, H. Li, and W. Chen, 2016, Seismic time-frequency analysis using bi-gaussian s transform: 78th Annual International Conference and Exhibition, EAGE, Extended Abstracts, DOI: 10.3997/2214–4609.201601333.

Chopra, S., and K. Marfurt, 2007, Seismic attributes for prospect identification and reservoir characterization: SEG.

Daubechies, I., 1992, Ten lectures on wavelets: Society for Industrial and Applied Mathematics.

Daubechies, I., J. Lu, and H.-T. Wu, 2011, Synchrosqueezed wavelet transforms: An empirical mode decomposition-like tool: Applied and Computational Harmonic Analysis, **30**, 243–261.

Fisher, G., D. Hunt, A. Colpaert, B. G. Wall, and J. Henderson, 2010, Comprehensive karst delineation from 3D seismic data: AAPG GEO 2010 Middle East Geoscience Conference & Exhibition, March 7–10, 2010 – Manama, Bahrain.

Fomel, S., 2013, Seismic data decomposition into spectral components using regularized nonstationary autoregression: Geophysics, **78**, O69–O76.

Ford, D. C., and P. W. Williams, 1989, Karst geomorphology and hydrology: London, Unwin Hyman,, 562.

Han, J., and M. van der Baan, 2013, Empirical mode decomposition for seismic time-frequency analysis: Geophysics, **78**, O9–O19.

Hardage, B. A., D. L. Carr, D. E. Lancaster, J. L. Simmons, R. Y. Elphick, V. M. Pendleton, and R. A. Johns, 1996a, 3-D seismic evidence of the effects of carbonate karst collapse on overlying clastic stratigraphy and reservoir compartmentalization: Geophysics, **61**, 1336–1350.

Hardage, B. A., D. L. Carr, D. E. Lancaster, J. L. Simmons, D. S. Hamilton, R. Y. Elphick, K. L. Oliver, and R. A. Johns, 1996b, 3-D seismic imaging and seismic attribute analysis of genetic sequences deposited in low accommodation conditions: Geophysics, **61**, 1351–1362.

Lin, T., Z. Wan, B. Zhang, S. Guo, K. Marfurt, and Y. Guo, 2013, Spectral decomposition of time- vs. depth-migrated data: SEG expanded abstracts:83rd Annual international meeting, 1384–1388.

Liu, G., S. Fomel, and X. Chen, 2011a, Time-frequency analysis of seismic data using local attributes: Geophysics, **76**, P23–P34.

———, 2011b, Time-frequency analysis of seismic data using local attributes: Geophysics, **76**, P23–P34.

Liu, J., and K. J. Marfurt, 2007, Instantaneous spectral attributes to detect channels: Geophysics, **72**, P23–P31.

Liu, W., S. Cao, and Y. Chen, 2016a, Application of variational mode decomposition in random noise attenuation and time-frequency analysis of seismic data: 78th Annual International Conference and Exhibition, EAGE, Extended Abstracts.

———, 2016b, Applications of variational mode decomposition in seismic time-frequency analysis: Geophysics, in press.

———, 2016c, Seismic time-frequency analysis via empirical wavelet transform: IEEE Geoscience and Remote Sensing Letters, **13**, 28–32.

Nissen, S. E., T. R. Carr, and K. J. Marfurt, 2005, Using new 3-d seismic attributes to identify subtle fracture trends in mid-continent mississippian carbonate reservoirs: Dickman field, kansas: AAPG Annual Convention Calgary.

Nordli, C., 2009, Fluid flow in and around collapsed karst structures; breccia pipes, in petroleum reservoirs: Master thesis, Centre of Integrated Petroleum Research.

Pinnegar, C. R., and L. Mansinha, 2003, The s-transform with windows of arbitrary and varying shape: Geophysics, **68**, 381–385.

Pollastro, R. M., D. M. Jarvie, R. J. Hill, and C. W. Adams, 2007, Geologic framework of the Mississipian Barnett Shale, Barnett-Paleozoic total petroleum system, Bend-arch–Fort Worth Basin, Texas: AAPG Bulletin, **91 (4)**, 405–436.

Reine, C., M. van der Baan, and R. Clark, 2009, The robustness of seismic attenuation measurements using fixed- and variable-window time-frequency transforms: Geophysics, **74**, 123–135.

Rodriguez, I. V., D. Bonar, and M. Sacchi, 2012, Microseismic data denoising using a 3c group sparsity constrained time-frequency transform: Geophysics, **77**, V21–V29.

Stockwell, R. G., L. Mansinha, and R. P. Lowe, 1996, Localization of the complex spectrum: The s transform: IEEE Transactions on Signal Processing, **44**, 998–1001.

Wang, Y., W. Lu, and P. Zhang, 2015, An improved coherence algorithm with robust local slope estimation: Journal of Applied Geophysics, **114**, 146.

Xie, Q., Y. Chen, G. Zhang, S. Gan, and E. Wang, 2015a, Seismic data analysis using synchrosqueezeing wavelet transform - a case study applied to boonsville field: 77th Annual International Conference and Exhibition, EAGE, Extended Abstracts, DOI: 10.3997/2214–4609.201412752.

Xie, Q., B. Di, Y. Chen, S. Gan, and S. Jiao, 2015b, Simultaneous structure enhancing filtering and fault detection using plane wave prediction: 77th Annual International Conference and Exhibition, EAGE, Extended Abstracts, DOI: 10.3997/2214–4609.201412614.

Zhang, C., Y. Li, H. Lin, and B. Yang, 2015a, Simultaneous denoising and preserving of seismic signals by multiscale time-frequency peak filtering: Journal of Applied Geophysics, **117**, 42–51.

Zhang, D., S. Z. Sun, H. Liu, and P. F. Wang, 2016, Complex carbonate reservoir characterization based on synchrosqueezing wavelet transform: 78th Annual Interna-

tional Conference and Exhibition, EAGE, Extended Abstracts, DOI: 10.3997/2214–4609.201601389.

Zhang, G., Z. Wang, Y. Sun, and Y. Chen, 2015b, Characterization method of tight dolomitic reservoir of fengcheng formation in the west slope of mahu sag, junggar basin, china: SEG expanded abstracts: 85th Annual international meeting, 2896–2900.